



The Effect of Mesenchymal Stem Cells Derived-Conditioned Media in Combination with Oral Anti-Androgenic Drugs on Male Pattern Baldness: An Animal Study

Majid Kamali-Dolat Abadi, M.Sc.¹, Gholamhossein Yousefi, Ph.D.², Farzaneh Dehghani, Ph.D.^{3,4}, Ali Akbar Alizadeh, Ph.D.¹, Abolfazl Jangholi, M.Sc.⁵, Mohammad Amin Moadab, B.Sc.⁶, Maryam Naseh, Ph.D.³, Shima Parsa, M.D.⁷, Golara Nasiri, Ph.D.⁸, Negar Azarpira, M.D., Ph.D.^{7*} , Mehdi Dianatpour, Ph.D.^{9,10*} 

1. Department of Tissue Engineering and Applied Cell Sciences, School of Advance Medical Science and Technology, Shiraz University of Medical Sciences, Shiraz, Iran
2. Department of Pharmaceutics, School of Pharmacy, Shiraz University of Medical Sciences, Shiraz, Iran
3. Histomorphometry and Stereology Research Center, Shiraz University of Medical Sciences, Shiraz, Iran
4. Department of Anatomical Sciences, School of Medicine, Shiraz University of Medical Sciences, Shiraz, Iran
5. Department of Biology, Faculty of Science, Razi University, Kermanshah, Iran
6. Department of Biology, Zand Institute of Higher Education, Shiraz, Iran
7. Transplant Research Center, Shiraz University of Medical Sciences, Shiraz, Iran
8. Department of Tissue Engineering and Cell Therapy, School of Advanced Technologies in Medicine, Shiraz University of Medical Sciences, Shiraz, Iran
9. Stem Cell Technology Research Center, Shiraz University of Medical Sciences, Shiraz, Iran
10. Department of Medical Genetics, School of Medicine, Shiraz University of Medical Sciences, Shiraz, Iran

Abstract

Objective: Androgenetic alopecia (AGA) is a prevalent form of hair loss, mainly caused by follicular sensitivity to androgens. Despite developing different anti-androgen treatment options, the success rate of these treatments has been limited. Using animal models, this study evaluated the therapeutic effects of umbilical cord (UC) stem cell conditioned media (CM) combined with oral anti-androgens for hair regeneration.

Materials and Methods: In this experimental study, Poloxamer 407 (P407) was used as a drug carrier for subcutaneous testosterone injection. AGA models were treated with oral finasteride, oral flutamide, and CM injections. Samples were thoroughly evaluated and compared using histological, stereological, and molecular analyses.

Results: Injecting CM-loaded hydrogel alone or combined with oral intake of anti-androgens improved hair regeneration. These treatments could promote hair growth by inducing hair follicles in the anagen stage and shortening the telogen and catagen phases. Furthermore, the combination treatment led to an upregulation of hair induction gene expression with a downregulation of inflammation genes.

Conclusion: Through a reduction in inflammation, injection of CM-loaded hydrogel alone or combined with oral intake of anti-androgens induces the hair cell cycle with regeneration in damaged follicles. Hence, this could be a promising therapeutic method for AGA patients.

Keywords: Androgenetic Alopecia, Conditioned Media, Finasteride, Flutamide, Mesenchymal Stem Cells

Citation: Kamali-Dolat Abadi M, Yousefi Gh, Dehghani F, Alizadeh AA, Jangholi A, Moadab MA, Naseh M, Parsa Sh, Nasiri G, Azarpira N, Dianatpour M. The effect of mesenchymal stem cells derived-conditioned media in combination with oral anti-androgenic drugs on male pattern baldness: an animal study. Cell J. 2023; 25(11): 790-800. doi: 10.22074/CELLJ.2023.2008138.1377

This open-access article has been published under the terms of the Creative Commons Attribution Non-Commercial 3.0 (CC BY-NC 3.0).

Introduction

Androgenetic alopecia (AGA) is the most prevalent form of hair loss affecting 80% of men and 50% of women over their lives. AGA is influenced by androgen and characterized by persistent, gradual and patterned hair thinning in defined areas of the scalp. Genetic inheritance and androgen levels are two major risk factors for AGA (1). Notably, the binding of dihydrotestosterone (DHT), a

metabolite of testosterone, to the androgen receptor (AR) is a crucial factor in the pathogenesis of this condition. As DHT accumulates in androgen-sensitive tissues, a progressive shrinking and thinning of the affected areas occur, eventually leading to alopecia (2). Despite AGA's prevalence and adverse effects, there is currently no universally accepted treatment for this condition. Drug therapies and follicular unit transplantation are routine treatment options for AGA. However, these treatment

Received: 30/July/2023, Revised: 16/September/2023, Accepted: 07/October/2023

*Corresponding Addresses: P.O.Box: 7193635899, Transplant Research Center, Shiraz University of Medical Sciences, Shiraz, Iran

P.O.Box: 7134845794, Department of Medical Genetics, School of Medicine, Shiraz University of Medical Sciences, Shiraz, Iran

Emails: azarpiran@sums.ac.ir, dianatpour@sums.ac.ir



Royan Institute
Cell Journal (Yakhteh)

options cannot cure AGA effectively and permanently (3). Therefore, it is essential to develop novel therapeutic strategies to discover more effective treatment options.

The use of AR antagonists presents a potential therapeutic approach for AGA. Flutamide, a nonsteroidal anti-androgen drug, was shown to block the action of both endogenous and exogenous testosterone through binding to AR (4). Finasteride is the first food and drug administration (FDA)-approved oral treatment for AGA which acts through selective inhibition of type II 5 α reductase. Finasteride reduces follicular shrinkage by irreversibly binding to the enzyme and blocking the production of DHT from testosterone (5). While flutamide, finasteride, and other chemical drugs are used as primary alopecia therapies, their potential synergistic effects and undesirable side effects have remained unclear (6).

The dermal papilla (DP) of the hair follicle (HF) is a critical signalling region responsible for sustaining hair development, regulating hair formation and cycling by paracrine secretion (7). Accordingly, a poor DP microenvironment may lead to hair loss. Additionally, androgen-induced changes in autocrine or paracrine compounds of DP cells are associated with HF stem cell dysfunction (8). In this regard, regenerative medicine using cell products and tissue engineering can be a suitable treatment for hair loss. Treatments based on cell therapy are among the suggested approaches, which play an essential role in migrating endothelial cells, fibroblasts and skin cells due to proliferation intensifiers (9). Stem cell therapy is a new technique for treating hair loss (HL) using exogenous cell sources or progenitor cells (PCs), such as follicular stem cells and the umbilical cord (UC) that are used in clinical trials (10). Another approved regenerative medicine method is thermo-sensitive gel products, a simple, low-cost method with a slow-release property (11). Poloxamer 407 (P407) system is a thermo-sensitive and high-quality carrier in drug delivery. P407 is in the form of a gel at a temperature close to the body (37°C) and remains as a stable carrier at the injection site (12). In addition, several studies have shown that conditioned media (CM) can influence hair stem cell activation and angiogenesis, accelerated hair density, and increased volume in AGA patients (13, 14). Indeed, dental pulp stem cells-derived CM (dental-MS) have the ability to activate hair follicles, neural cells, adipocytes, and dentin-producing cells (13).

In the embryonic ectoderm germ layer, these multipotent cells originate from temporary neural crest cells. The ability of these stem cells to differentiate into other cells may make them useful in the treatment of different disorders. Furthermore, CM contains multiple growth factors released by stem cells, which may be effective in repairing tissue under different conditions (15).

Mesenchymal stem cells (MSCs), immature precursors derived from the mesoderm, possess self-renewal capabilities and the capacity for multilineage differentiation. Studies have demonstrated that paracrine

factors secreted in CM are primarily responsible for the therapeutic activity observed in MSC. In CM therapy, extracellular vesicles (EVs) and soluble factors are transferred to activate signalling pathways. EVs contain various components including mRNAs, miRNA, growth factors and cytokines. Retrospective human studies have demonstrated that CM regulates the hair cycle and the regeneration of hair follicles.

Early hair regression is thought to be caused by DHT, a hormone derived from testosterone. Moreover, it was found that it reduced the volume of the cellular hair matrix and reduced the duration of the anagen growth phase in genetically susceptible hair follicles. The DHT synthesis inhibitor (DHT-inhibitor) is regarded as one of the most important metabolites in hair development, although it is not able to completely alleviate hair loss. Despite this, long-term treatment of AGA with DHT inhibitors has been documented in well-controlled clinical trials to be both effective and safe. As reported by Kamishima et al. (13), androgen inhibitors are quite beneficial, especially when started at an early stage of the disease.

In this study, CM, a mixture of growth factors and peptides derived from stem cells, was loaded in P407 thermosensitive hydrogel and injected into the alopecia-induced mice model. The effects of CM-rich P407 thermosensitive gel in combination with oral anti-androgens on hair growth and its inhibitory effect on hair loss at the molecular level were investigated. In addition, we examined two forms of AGA strategy with different natures, the first one is anti-androgens, and the second one is based on cell therapy.

Materials and Methods

Isolation and characterization of human umbilical cords mesenchymal stem cells

This experimental study was approved by the Shiraz University of Medical Sciences Ethics Committee (IR.SUMS.REC.1398.855). After obtaining written informed consent, UCs were collected from women (18 to 30 years old) who underwent cesarean section. The cords were cultured in a culture plate containing minimum essential medium eagle-alpha modification (Alpha MEM) (Shellmax, USA) supplemented with 10% fetal bovine serum (FBS, Gibco, Life, USA) and 1% penicillin-streptomycin at 37°C with 5% CO₂. The culture medium was changed every three days (16). Cell surface markers, including HLADR, CD44, CD90, and CD34, were analyzed using a FACSCalibur™ flow cytometer (Becton Dickinson, USA) to confirm the isolated cells. The certainty of the mesenchymal origin of cells was also evaluated by differentiation into osteoblasts and adipocytes using each specific differentiation medium (Gibco Life, USA) (17).

Preparation of condition media

Cells were selected, trypsinized (0.25%) and cultured in DMEM/F-12 (Shellmax, USA) supplemented with

10% FBS until 70 to 80% confluency. After 48 hours of incubation in a serum-free medium, CM was harvested. The media was collected, spun at 1000 rpm for 5 minutes to remove cell debris, and filtered through a 0.22 µm syringe filter, then freeze-dried, and stored at -20°C.

Preparation of thermo-sensitive Poloxamer 407 (P407) System

Injectable thermosensitive P407 was used as a testosterone carrier for sustained-release drug delivery. The P407 powder was dissolved at a concentration of 21% in phosphate-buffered saline (PBS) and Ethanol with a volume ratio of 80/20. Then, a testosterone injection solution (ALL-TEST-2433) was added to the P407 gel at a 5 gr/ml ratio. This solution was used in the early stages of the study to induce alopecia in animals. Furthermore, P407 maintained the slow release of umbilical cord MSC-CM (UC-MSc-CM). To achieve this, a suitable amount (200 µg) of dried CM was dissolved in P407 gel without ethanol to reach a concentration of 22% at 15°C (12, 18).

Evaluating the release rate of testosterone and conditioned media loaded in the gel

UV spectroscopy was used to analyze the *in vitro* release profiles of P407-CM and P407-testosterone. The *in vitro* release of CM and testosterone was investigated by placing two vials with known concentrations of P407-CM and P407-testosterone in a shaker incubator at 37°C for 15 minutes until a gel formed. After that, 1.5 ml of phosphate buffer (pH=7.4) was added to each container. The samples were obtained at specified time intervals (periods), replaced with the same volume of pre-warmed fresh PBS, and centrifuged for 15 minutes at 12000 rpm. The absorbance was recorded at 240 nm using a UV-visible spectrophotometer. The Bradford assay was also used to assess the concentration of CM (18, 19).

Animal groups

Six-week-old male C57BL/6 mice (35-50 g) were acquired from the Shiraz University of Medical Sciences Animal Lab. For each group, six male mice were placed into separate cages to prevent interference between them. The housing and handling of mice were conducted based on the Ethics Committee guidelines in cages at ambient temperature (25 ± 2°C), and the mice were fed standard mouse chow and water ad libitum under light/dark cycles of 12 hours and 12 hours. Dorsal skin hair was shaved in 48 mice, and they were categorized into eight groups as listed in Table 1. Then subcutaneous injection of testosterone with Poloxamer 407 (P407) carrier was used to induce alopecia in mice. For injection, 0.2 ml of gel containing 2 mg of CM was used in two stages on days 1 and 21. The mice were evaluated daily for changes in hair loss and growth, and the photographs were taken in

the first and last days of the study. Finally, the mice were sacrificed 42 days after the start of the study (14, 20).

Table 1: Classification of studied mice for different treatments

Groups	Treatment
PBS	PBS=every 4 days
P407	P407=every 4 days
P.T	P.T=every 4 days
CM	P.T=every 4 days, CM=Day 1 and 21 of the study
Fl	P.T=every 4 days, Fl=everyday
CM.Fl	P.T=every 4 days, Fl=everyday, CM=Day 1 and 21 of the study
Fin	P.T=every 4 days, Fin=everyday
CM.Fin	P.T=every 4 days, Fin=everyday, CM=Day 1 and 21 of the study

PBS; Phosphate-buffered saline, P407; Poloxamer 407, P.T; Poloxamer 407+Testosterone, CM; Poloxamer 407+umbilical cord stem cell conditioned media, Fl; Oral flutamide, and Fin; Oral finasteride.

Anti-androgenic treatment

Flutamide and finasteride, an androgen antagonist and a 5-alpha reductase inhibitor, respectively, were utilized as oral anti-androgenic drugs (Table 1). The mice were fed daily with flutamide at a dose of 1.75 g/ml in soybean oil and finasteride at a concentration of 0.007 mg/ml in water.

Excisional biopsy and sample preparation

On the final day of the experiment, animals were sacrificed for histological, stereological, and molecular analysis. Samples were collected from the area between 0.5-1 mm below the dermo-epidermal junction.

Stereological analysis

A full-thickness dorsal skin sample (2×2 cm²) was removed and subsequently fixed in buffered formaldehyde for stereological assessment. The specimen was sectioned into 0.5×0.5 cm², and nine pieces were selected according to the systematic random sampling method. Using a microtome, the sample pieces were embedded in a paraffin block and sectioned with 5 µm and 20 µm thickness. Then, Heidenhain's Azan trichrome and hematoxylin-eosin were used to stain 5 µm and 20 µm sections, respectively (Fig.1A, B).

Estimation of the volume density

Microscopic skin analyses were carried out by a video-microscopy system (Nikon E-200, Tokyo, Japan). The point-counting method was utilized to estimate the volume densities of the dermis, epidermis, hypodermis, collagen bundles, and vessels. Briefly, a point grid was superimposed on the images of the 5 µm thickness skin

on the monitor using stereology software designed by Shiraz University of Medical Sciences, Shiraz, Iran (Fig.1A). The volume density (Vv) was measured using the following formula (21):

$V_v(\text{structure, reference}) = \Sigma P(\text{structure}) / \Sigma P(\text{reference})$
Where " $\Sigma(\text{reference})$ " and " $\Sigma P(\text{structure})$ " are the whole skin sections and the total points hitting the favoured structures, respectively.

Estimation of the numerical density

To obtain the numerical density (number of the cells per unit volume of the dermis; Nv) of the fibroblasts, the 20 μm slides were analyzed using the "optical dissector" method (Fig.1B), and Nv was calculated using the following formula (15):

$$N_v = [\Sigma Q / \Sigma P \times a / f \times h] \times [t / BA]$$

where " ΣQ " represents the total number of cells counted during scanning the section thickness (on average, 700 neurons and 600 oligodendrocytes per animal), " ΣP " is the total number of counting frames in all fields (130 frames per animal, on average), "a/f" and "h" are the frame area and the height of the dissector, respectively. "BA" is the block advance of the microtome (30 μm) and "t" refers to the real post-processing section thickness calculated using the microcator (25 μm). To calculate the total number of cells, the numerical density (NV) was multiplied by the reference volume (V).

Histopathology study

The biopsy sample was fixed in a 10% formalin fixative solution, embedded in paraffin, and sectioned into 3 μm thick slices for histopathology evaluation. HFs in different stages of catagen, telogen, and anagen were counted. The count was done in 10 different fields (40x) and mean \pm SD was calculated for each parameter. Compared to normal skin, any change in the number of HFs and a difference in the inflammatory reaction was considered as an intervention effect. The stage of HF growth (Anagen, Telogen and Catagen) and hair type (vellus or terminal) were evaluated.

Quantitative gene analysis

Total RNA from the treated skin tissue was extracted using the AddPrep Total RNA Extraction Kit (Addbio, Korea) based on the manufacturer's instructions. The concentration and purity of RNA were quantified using a NanoDrop ND-1000 spectrophotometer (NanoDrop Technologies, Wilmington, DE, USA). Next, cDNA was synthesized (Addbio, Korea) and used as a template for a real-time polymerase chain reaction (PCR). After cDNA synthesis, the expression of *Il-1 β* , *Il-1 α* , *Tnf- α* , *Lef-1*, *Versican*, and *Ptc-1* genes along with Beta-actin (*β -actin*) as an internal control was measured using real-time PCR. For this purpose, specific gene primers and 2x Q-PCR Master Mix SYBER GREEN Add SYBR Master

kit were used based on the manufacturer's protocol. The relative expression of the mRNA was quantified using the comparative cycle threshold method. The following primer sequences were used:

β -Actin-

F: CAGCTGAGAGGGGAAATCGTG

R: CGTTGCCAATAGTGATGACC

Il-1 β -

F: ACAAGGAGAACCAAGCAACGAC

R: GCTGATGTACCAGTTGGGGAAC

Il-1 α -

F: CTGTGCCTGTCTTGTGCCA

R: AGAGCGGATGAAGGTAAGCG

Tnf- α -

F: TGCCCCAAGGACACCCC

R: GGGCTGGGTAGAGAATGGATGA

Lef-1-

F: ACCGATGAGATGATCCCCCT

R: CCTCTTCGGGATGACTGAT

Versican-

F: TTTTACCCGAGTTACCAGACT

R: AGTAGTTGTTACATCCGTTGC

Ptc-1-

F: ACATTCAAAGAAGAACTGCGGC

R: AAAGGGAAGGAAGACGAAGG

Statistical analysis

The data was presented as mean \pm SD. GraphPad Prism software (version 8.0, La Jolla, CA) was used to generate all the graphs. The groups were analyzed using One-way ANOVA and Tukey's tests using GraphPad (Version 8.0, La Jolla, CA). Differences were reported as statistically significant if $P < 0.05$.

Results

Characterization of human umbilical cords mesenchymal stem cells and the hydrogel

To confirm the mesenchymal origin of cells, isolated cells were evaluated by differentiation into osteoblasts and adipocytes. The presence of calcium deposits indicated the potential of cells to become osteoblasts, while the presence of intracellular lipid vacuoles was noted as a distinguishing characteristic of adipocytes (17). Cells were also characterized by flow cytometry using different surface markers. The presence of positive markers, CD90 and CD44, and the absence of negative markers, HLA-DR and CD34 were confirmed on the isolated cells (Fig.1C-F).

We also evaluated the release of CM and testosterone from the gel system. We observed that CM was released from the gel system after 20 days (Fig.1G). However, approximately 60% of the testosterone was released within the first 24 hours, with complete release occurring within 160 hours (Fig.1H).

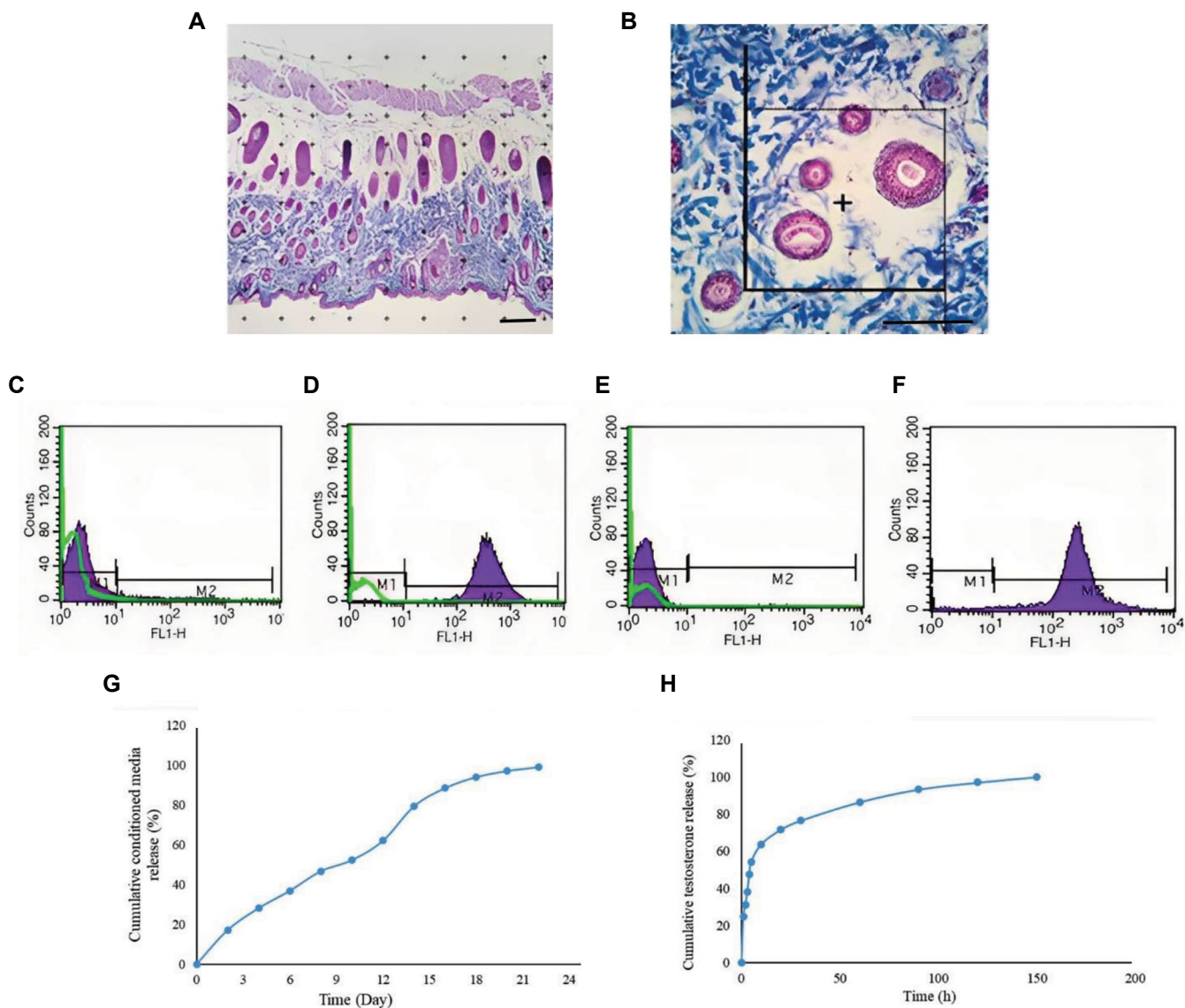


Fig.1: A schematic representation of stereological methods was used in this study. **A.** Point-counting method for calculating volume density, **B.** Optical disector method for estimating numerical density (scale bar: 50 μ m). The ability of human UC-MSCs differentiation into adipocytes and osteocytes. Immunophenotyping analysis of UC-MSCs. Cells were positive for **C.** CD44, **D.** CD99 and negative for **E.** HLA-DR, **F.** CD34. The control histogram is highlighted in green. CM and testosterone release rate loaded in the hydrogel. **G.** Cumulative CM release and **H.** Cumulative testosterone release. UC-MSCs; umbilical cords mesenchymal stem cells and CM; Conditioned media.

Gross, histopathological and stereological evaluations of the treated groups

The results of gross and histopathological studies showed the increase and regeneration of HF in all treatment groups (Figs.2A-H, 3A-C). CM.FI and CM.Fin treatment resulted in the most significant effect on the anagen phase, leading to an earlier onset and a longer duration of HF growth. Regarding the HF cycle, in CM, CM.FI and CM.Fin treated groups, the number of HF in the telogen and catagen phases were greatly reduced. The combination of CM with flutamide displayed a significant improvement in promoting HF toward the anagen phase ($P < 0.05$).

AGA is characterized by the presence of small-sized

hair follicles and a shortening anagen phase Figure 2CIII (22). Hair loss typically correlates with irregularities in HF cycling and morphology, as shown in Figure 2CIII. During the anagen state of a hair follicle, DP remains situated deep within the subcutaneous fat layer, as depicted in Figure 2CIII (23). In addition, the number of vellus and terminal hairs was evaluated between groups. Across all treated groups, vellus hairs decreased, while terminal hairs increased (Fig.3D, E). However, CM, CM.FI, and CM.Fin treated groups demonstrated a higher level of terminal hairs compared to other treated groups. Similarly, the groups treated with CM showed a significant reduction of inflammation ($P < 0.05$, Fig.3F) (24).

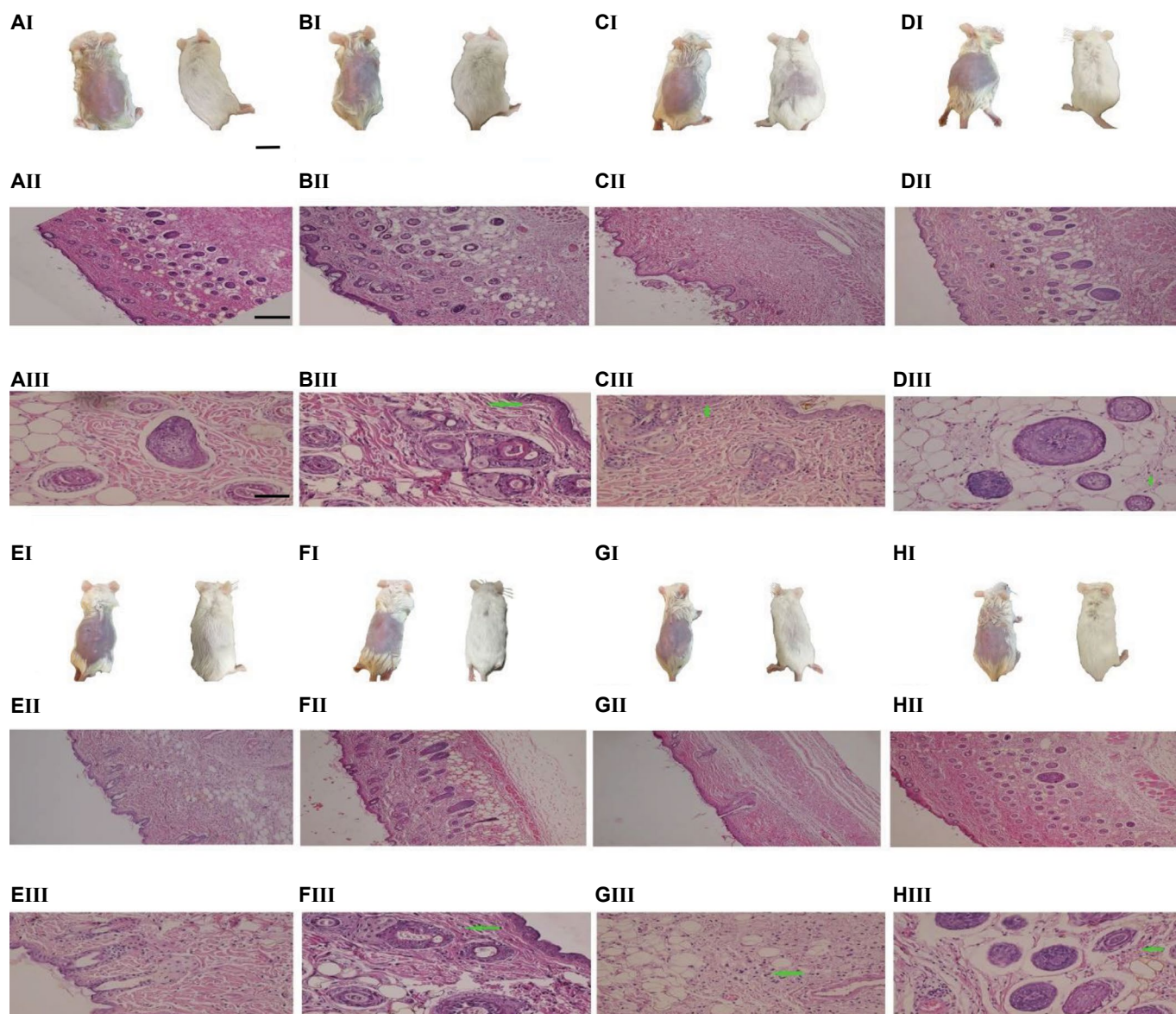


Fig.2: The gross appearance of alopecia and hematoxylin and eosin staining of HF in different treatment groups. The mice were treated using **A.** PBS, **B.** P407, **C.** P.T, **D.** C.M, **E.** FI, **F.** CM.FI, **G.** Fin, and **H.** CM.Fin. The presented photographs depict the first (left) and last (right) days of the experiment (AI-HI) (scale bar: 1 cm). AII-HII 100x (scale bar: 50 μ m). AIII-HIII 400x-Green arrow showing inflammation (scale bar: 200 μ m). HF; Hair follicle, PBS; Phosphate-buffered saline, P407; Poloxamer 407, P.T; Poloxamer 407+Testosterone, C.M; Poloxamer 407+Testosterone)+(Poloxamer 407+conditioned media), F1; (Poloxamer 407+Testosterone)+(Oral flutamide, CM), F1; (Poloxamer 407+Testosterone)+(Oral flutamide), Fin; (Poloxamer 407+Testosterone)+(Oral finasteride), and CM.Fin; (Poloxamer 407+Testosterone)+(Oral finasteride)+ (Poloxamer 407+conditioned media).

As shown in Figure 3, a significant difference in the volume density of the epidermis between the P.T and PBS treated groups was found ($P < 0.05$). There was also a significant difference in hypodermis between the P.T and PBS treated groups ($P < 0.05$). Although, CM, CM.FL and CM.Fin treatments could significantly prevent subcutaneous layer loss ($P < 0.05$), no significant changes in dermal volume density were observed.

As a result of treatment with P.T, FL, or Fin, collagen volume density was significantly reduced in comparison with the PBS treated group ($P < 0.05$), whereas the CM, CM.FI, and CM.Fin treated groups demonstrated significant increases in this parameter ($P < 0.05$, Fig.3J). The volume density of vessels was reduced

in the P.T, FL and Fin treated groups compared to the control group ($P < 0.001$). Moreover, it was shown that the volume densities of vessels in the CM, CM.FI, and CM.Fin groups were significantly higher than the P.T group ($P < 0.001$). Interestingly, a significant difference was seen between the FI and Fin treated animals and the CM treated group ($P < 0.01$). Combined groups with CM improved the Vessel's volume density more than either FI or Fin groups ($P < 0.001$, Fig.3K).

Conversely, the volume density of the sebaceous gland was increased in the P.T ($P < 0.001$), FL and Fin treated groups ($P < 0.01$) compared to the Control group. This parameter was reduced in the FL and Fin-treated mice ($P < 0.05$), as well as CM, CM.FI, and CM.Fin treated groups ($P < 0.001$) compared to the P.T group (Fig.3L).

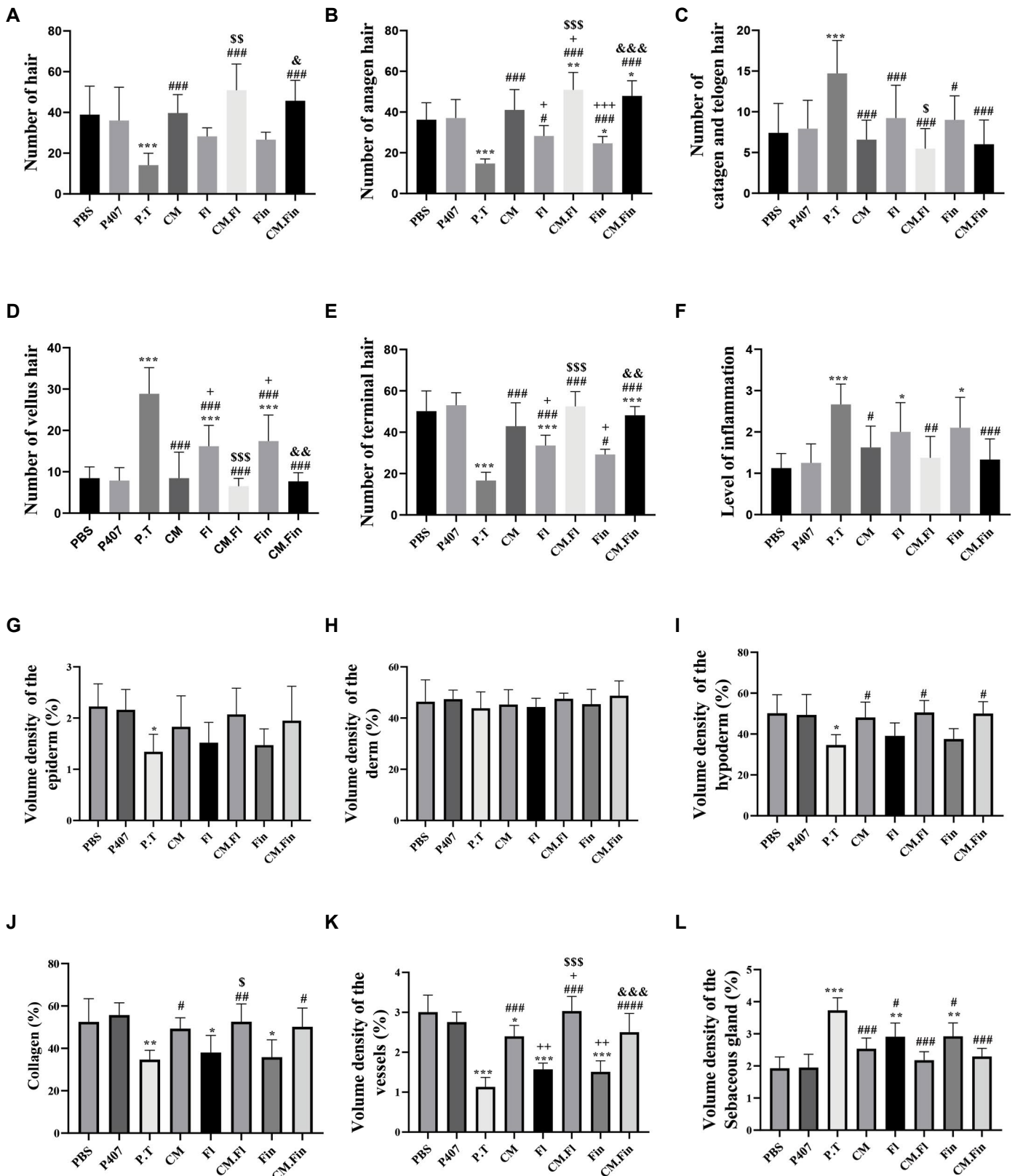


Fig.3: The effect of anti-androgen treatments and regenerative medicine on the hair follicle cycle and components of skin layers in mice. **A.** Quantitative analysis of the number of hair follicles, **B.** The number of follicles in the anagen phase, **C.** The number of follicles in the catagen or telogen phase, **D.** The number of vellus hairs, **E.** The number of terminal hairs, and **F.** The degree of inflammation. **G.** The volume density (%) of skin's layers including epidermis, **H.** Dermis, **I.** Hypodermis among the treated groups. **J.** The volume density (%) of the collagen bundle, **K.** Vessels, and **L.** Sebaceous gland in the experimental groups. Data are presented as n=6 ± SD. HF; Hair follicle, PBS; Phosphate-buffered saline, P407; Poloxamer 407, P.T; (Poloxamer 407+Testosterone), C.M; (Poloxamer 407+Testosterone)+(Poloxamer 407+conditioned media), F1; (Poloxamer 407+Testosterone)+(Oral flutamide), CM.F1; (Poloxamer 407+Testosterone)+(Oral flutamide)+(Poloxamer 407+conditioned media), Fin; (Poloxamer 407+Testosterone)+(Oral finasteride), CM.Fin; (Poloxamer 407+Testosterone)+(Oral finasteride)+(Poloxamer 407+conditioned media), *, P<0.05, **, P<0.01, ***, P<0.001 vs. the PBS group, #; P<0.05, ##; P<0.01, ###; P<0.001 vs. the P.T group, +; P<0.05, ++; P<0.01 vs. the CM group, +++; P<0.001 vs. the CM group, \$; P<0.05, \$\$; P<0.01, \$\$\$; P<0.001 vs. the FI group, &; P<0.05, &&; P<0.01, and &&&; P<0.001 vs. the Fin group.

The stereological data obtained for HFs and components of HFs, including medulla, cortex, inner root sheath, outer root sheath, and dermal root sheath, are listed in Table 2. The volume density of all parameters was reduced in the P.T. group in comparison to the PBS-treated animals ($P < 0.05$). These components were significantly increased in mice treated with CM, CM.FI, and CM.Fin compared to P.T group ($P < 0.05$).

As shown in Table 2, the numerical density of spinous cells in the epidermis and fibroblasts in the dermis of the P.T, FL, and Fin treated mice were lower than the PBS treated group ($P < 0.001$). These cells were significantly increased in the CM ($P < 0.01$), CM.FI, and CM.Fin treated groups ($P < 0.001$) compared to the P.T treated group. In addition, a significant difference was observed between the CM.FI and CM.Fin treated animals and CM group ($P < 0.01$). No significant

changes were found in the numerical density of basal cells between groups. Taken together, CM.FI and CM.Fin could improve the numerical density of these cells more than either FI or Fin groups ($P < 0.001$) (25).

Gene expression analysis

The expression of *Il-1 α* , *Il-1 β* , and *Tnf- α* genes were up-regulated in the alopecic models compared to the control group (Fig.4A-C). Following treatment, the expression of these genes was decreased in all groups. However, a significant reduction was found in the groups treated by CM, CM.FI, and CM.Fin compared to the other groups. A decrease in the expression of genes related to hair growth and survival, *Ptc1*, *Versican*, and *Lef* are closely associated with androgenic alopecia (Fig.4D-F). However, subsequent to treatment with CM, CM.FI, and CM.Fin, a significant upregulation of *Ptc1*, *Versican*, and *Lef* was observed within the respective groups. ($P < 0.05$).

Table 2: The mean and standard deviation of the volume density (%) of the HF and components of the HF in the experimental groups (n=6)

Group	Hair follicle (Vv)	Hair follicle component (Vv)					Fibroblast (Nv)	Epidermis cells (Nv)	
		Medulla	Cortex	Inner root sheath	Outer root sheath	Dermal root sheath		Basal	Spinousum
PBS	6.213 ± 1.205	3.750 ± 0.3852	6.120 ± 1.776	15.63 ± 3.588	31.93 ± 3.064	7.859 ± 1.789	176.7 ± 17.07	175.2 ± 28.13	533.6 ± 93.64
P407	6.400 ± 1.071	3.512 ± 0.7372	5.821 ± 1.355	15.73 ± 4.923	31.00 ± 5.161	8.079 ± 2.139	188.1 ± 33.89	176.7 ± 28.25	517.2 ± 88.09
P.T	3.372 ± 0.4764*	1.775 ± 0.4453*	2.944 ± 1.442*	7.879 ± 3.330*	18.90 ± 4.901*	3.579 ± 0.8825*	70.46 ± 11.50***	161.4 ± 30.20	219.7 ± 47.07***
CM	6.244 ± 0.8346#	3.606 ± 0.9045#	5.501 ± 1.315#	13.46 ± 3.650	28.43 ± 4.058#	7.799 ± 2.024#	159.7 ± 27.88##	171.8 ± 24.67	360.8 ± 62.24##
FI	4.996 ± 0.2512#	2.867 ± 0.8659	3.720 ± 0.7429	10.74 ± 2.316	25.10 ± 6.805	5.876 ± 2.133	95.48 ± 11.62***	166.2 ± 15.13	277.1 ± 47.04***
CM.FI	6.548 ± 0.9315#	3.829 ± 1.275#	6.099 ± 1.658#	15.17 ± 2.374#	33.75 ± 5.961#	8.770 ± 2.748#	235.6 ± 24.28#####	176.0 ± 30.28	564.5 ± 94.20#####
Fin	4.951 ± 0.5134#	2.659 ± 1.162	3.938 ± 1.254	12.19 ± 1.922	26.19 ± 3.139	5.526 ± 1.527	94.78 ± 12.36***	167.3 ± 19.57	253.8 ± 38.32***
CM.Fin	6.324 ± 0.9461#	3.614 ± 1.090#	6.233 ± 1.155#	14.05 ± 1.280#	31.93 ± 4.068#	8.184 ± 2.460#	223.8 ± 29.10##### &&&	175.9 ± 19.03	565.0 ± 84.49##### &&&

The mean and standard deviation of the numerical density of fibroblasts, basal cells, and spinous cells ($\times 10^3$ per mm^3) in the experimental groups (n=6). *, $P < 0.05$ vs. the PBS group, #; $P < 0.05$ vs. the P.T group. ***, $P < 0.001$ vs. the PBS group, ##; $P < 0.01$, ###; $P < 0.001$ vs. the P.T group, +; $P < 0.01$ vs. the CM group, \$\$\$; $P < 0.001$ vs. the FI group, and &&&; $P < 0.001$ vs. the Fin group.

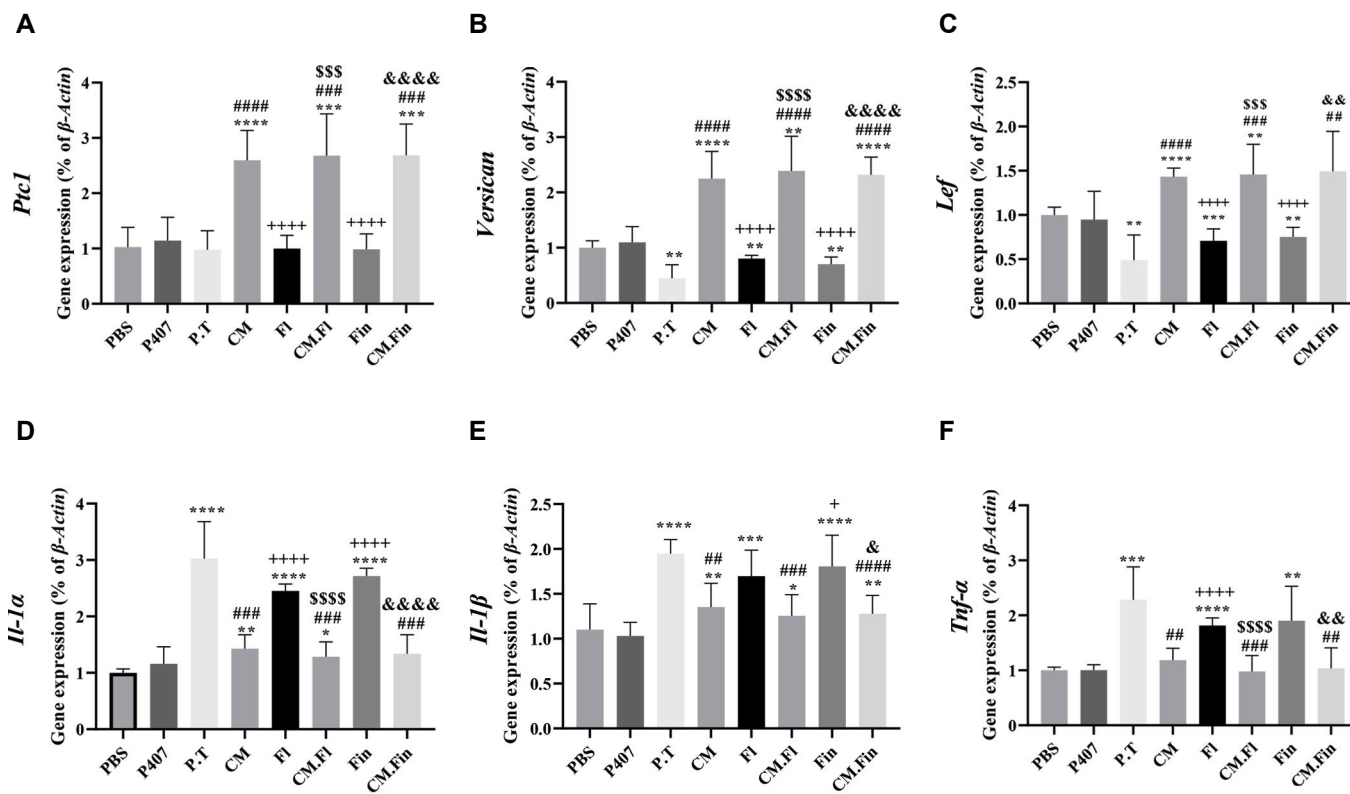


Fig.4: Expression of cytokine genes. **A. *Il-1 α*** , **B. *Il-1 β*** , and **C. *Tnf- α*** as well as growth and survival genes including, **D. *Ptc1***, **E. *Versican*** and **F. *Lef*** in different studied groups. Expression level of genes related to in different studied groups. *, P<0.05, **, P<0.01, ***, P<0.001, ****, P<0.0001 vs. the PBS group, ##, P<0.01, ###, P<0.001, ####, P<0.0001 vs. the P.T group, +, P<0.05, ++, P<0.001, +++, P<0.0001 vs. the CM group, \$\$\$, P<0.001, \$\$\$\$, P<0.0001 vs. the Fl group, &, P<0.5, &&, P<0.01, &&&, P<0.001, &&&&, P<0.0001 vs. the Fin group, PBS; Phosphate-buffered saline, P407; Poloxamer 407, P.T; (Poloxamer 407+Testosterone), C.M; (Poloxamer 407+Testosterone)+(Poloxamer 407+conditioned media), F1; (Poloxamer 407+Testosterone)+(Oral flutamide), CM.F1; (Poloxamer 407+Testosterone)+(Oral flutamide)+(Poloxamer 407+conditioned media), Fin; (Poloxamer 407+Testosterone)+(Oral finasteride), and CM.Fin; (Poloxamer 407+Testosterone)+(Oral finasteride)+ (Poloxamer 407+conditioned media).

Discussion

CM derived from MSCs contains bioactive factors that are involved in a wide variety of physiological processes, including cellular proliferation, angiogenesis, and hair growth. In CM, the proangiogenic component consists of HIF-1 α , hepatocyte growth factor (HGF), insulin-like growth factor-1 (IGF-1), fibroblast growth factor-2 (FGF-2), matrix metalloproteinase-2 (MMP-2) and CXCL5 (14).

A colony-stimulating factor, for example, may be capable of recruiting resident stem cells and/or PCs to facilitate hair regeneration. Overall, CM enhances angiogenesis and promotes hair regeneration in a complex and effective manner (14).

The present study evaluated the effects of CM-loaded hydrogel in combination with oral anti-androgen drugs on the histological and stereological changes in the mouse model of androgenetic alopecia. No side effects were observed in the control groups. We showed that CM-loaded hydrogel alone or combined with anti-androgen drugs improved hair regeneration by increasing HF, associated with increased densities of epidermis and hypodermis layers. An increased numerical density of fibroblasts with collagen bundles was also identified.

Furthermore, these treatments could promote hair growth by introducing HF in the anagen stage and shortening the telogen and catagen phases.

Hair growth can be induced by prolonged anagen and delayed catagen phases or by alternation from quiescent (telogen) to active (anagen) phases (26). It has been suggested that topical anti-androgenic compounds containing flutamide or finasteride could effectively stimulate hair growth in male-pattern baldness (27). Our result confirmed that flutamide and finasteride have been significantly successful in HF growth, and flutamide was more effective than finasteride. Other studies have shown flutamide to be effective in treating and preventing androgenic hair loss, especially in women (28), and the results obtained regarding the effectiveness of flutamide compared to finasteride in hair loss are in line with the results of this study. Moreover, localized supplementation of growth factors has been reported to promote hair regeneration and growth (29).

Previous studies have also shown that CM from Extracellular Matrix/Stromal Vascular Fraction Gel can promote hair growth by regulating the proliferation of DP cells and bulge cells, neovascularization and anagen induction in C57BL/6 mice (30). Lu et al. (31) stated

that an enriched culture medium contained effective proangiogenic elements and growth factors such as HIF-1 α , HGF, IGF-1, and FGF-2. Similarly, it has been reported that CM from vitamin D3 (Vd3) pre-activated preadipocytes have stimulatory effects on hair growth via the enhancement of angiogenesis in a hairless-induced C57BL/6 mouse model (32). Treatment of bone marrow MSCs with a Wnt1 α -conditioned medium accelerated the HF transition from the telogen to the anagen phase. Also, it activated DP cells and promoted mouse HF regrowth (33).

Oh et al. (22) showed that using an enriched culture medium obtained from UC stem cells pretreated with lithium chloride and TGF- β 1 significantly increased the thickness, growth rate, and number of HFs. In addition, HF-derived MSCs were able to decrease mouse hair loss and reduce inflammation around the HF(23). The concentrated conditioned medium-loaded hydrogel treatment accelerated wound closure, enhanced neovascularization, and promoted HF regeneration, which is in line with the results of this study (34). Nevertheless, to the best of our knowledge, the present study represents the first attempt to investigate the combination effects of CM-loaded hydrogel with flutamide or finasteride. The stereological analysis displayed that CM-loaded hydrogel alone or combined with oral intake of flutamide and finasteride could increase the numerical density of spinous cells, which may be the reason for the thickening of the epidermis. Our findings revealed that CM-loaded hydrogel alone or combined with flutamide and finasteride could also proliferate fibroblasts and improve collagen content. Fibroblasts are the main skin components that produce collagen and other matrix macromolecules for the structural support of connective tissues (35). Additionally, it has been reported that fibroblast proliferation could promote angiogenesis. Inconsistent with the findings here, Fong et al. (36) found that the enriched CM could significantly increase the cell life and total collagen, elastin, and fibronectin.

Liu et al. (37) determined that the enriched CM of stem cells increases collagen expression, activation, and migration of fibroblasts. Interestingly, combined treatment with CM significantly after exposure to testosterone reduced the volume density of sebaceous glands. It has been revealed that testosterone administration could increase the size of the sebaceous glands (38). Accordingly, despite the increase in fibroblasts and collagen content following combined treatment with CM, the lack of change in the dermis volume may be caused by a reduced sebaceous gland volume density. Medullation of the immune system with anti-inflammatory properties is another characteristic finding of stem cells and enriched CM (39). In this study, the enriched CM significantly reduced the expression of *interleukin 1 alpha*, *interleukin 1 beta*, and *Tnf alpha* genes. Accordingly, Deng et al. (23) showed that MSCs derived from HF can prevent hair loss by reducing inflammation. Also, Czarnecka et al. (40) stated that the immunoregulatory properties of

stem cells significantly increased hair growth. Expression of *ptc1*, *Versican*, and *lef1* genes activate the precocious anagen entry. Lef-1 plays an important role in regulating cell growth and differentiation through the Wnt signalling pathway. According to the results of this study, treatments with CM, CM.FI, and CM.Fin up regulates the expression of these genes and the Wnt/b-catenin signaling pathway promotes hair regeneration (33). Further investigations are needed to evaluate the protein profiles of the treated and control tissues and determine the effect of the treatment on the excessive or lessened expression of the proteins in the target tissue.

A significant advantage of this study is the identification of the therapeutic potential of regenerative medicine products in addition to conventional drugs for the treatment of androgenic hair loss. However, a genetic or animal model capable of accurately replicating AGA remains an area for further investigation. Future research should focus on the combination of CM with other drugs related to hair loss. Additionally, performing these experiments on other model animals may provide a better understanding of the quality of regenerative medicine treatments.

Conclusion

We have shown that the slow-release property of p407, which carries the therapeutic properties of CM at the injection site, provides a new treatment approach for male pattern hair loss. The injecting growth factors, anti-inflammatory and angiogenesis properties, in combination with oral anti-androgens, was found to be an optimal therapeutic strategy. Developing new effective treatments for this disease can be achieved by optimizing the injecting doses, type of cell therapy sources, and anti-androgen selections.

Acknowledgements

This study was funded by a grant from the Shiraz University of Medical Sciences [98-01-74-19509]. There is no conflicts of interest in this study.

Authors' Contributions

M.K.-D.A., N.A., M.D.; Conceptualization. M.K.-D.A., Gh.Y., F.D., A.A.A., M.A.M., G.N.; Methodology and Software. N.A., M.K.-D.A., A.J., S.P., M.N.; Data curation, Writing- Original draft preparation, and Supervision. M.K.-D.A., N.A., M.D., M.N.; Visualization and Investigation. N.A., M.D., M.N., F.D.; Software and Validation. M.K.-D.A., N.A., A.J., M.N., M.D.; Writing-Reviewing and Editing. All authors read and approved the final manuscript.

References

1. Devjani S, Ezemma O, Kelley KJ, Stratton E, Senna M. Androgenetic alopecia: therapy update. *Drugs*. 2023; 83(8): 701-715.
2. Ho CH, Sood T, Zito PM. Androgenetic alopecia. In: StatPearls [Internet]. Treasure Island (FL): StatPearls Publishing; 2023. Available from: <https://www.ncbi.nlm.nih.gov/books/NBK430924/> (16

- Oct 2022).
3. Lolli F, Pallotti F, Rossi A, Fortuna MC, Caro G, Lenzi A, et al. Androgenetic alopecia: a review. *Endocrine*. 2017; 57(1): 9-17.
 4. Anastassakis K. Flutamide. *Androgenetic alopecia from A to Z*. Springer; 2022; 193-197.
 5. Saceda-Corralo D, Domínguez-Santas M, Vañó-Galván S, Grimalt R. What's new in therapy for male androgenetic alopecia? *Am J Clin Dermatol*. 2023; 24(1): 15-24.
 6. Allam S, Elsakka EGE, Ismail A, Doghish AS, Yehia AM, Elkady MA, et al. Androgen receptor blockade by flutamide down-regulates renal fibrosis, inflammation, and apoptosis pathways in male rats. *Life Sci*. 2023; 323: 121697.
 7. Lei M, Yang L, Chuong CM. Getting to the core of the dermal papilla. *J Invest Dermatol*. 2017; 137(11): 2250-2253.
 8. Rahmani W, Abbasi S, Hagner A, Raharjo E, Kumar R, Hotta A, et al. Hair follicle dermal stem cells regenerate the dermal sheath, repopulate the dermal papilla, and modulate hair type. *Dev Cell*. 2014; 31(5): 543-558.
 9. Mohammadi P, Youssef KK, Abbasalizadeh S, Baharvand H, Aghdami N. Human hair reconstruction: close, but yet so far. *Stem Cells Dev*. 2016; 25(23): 1767-1779.
 10. Krefft-Trzcieniecka K, Piętowska Z, Nowicka D, Szepletowski JC. Human stem cell use in androgenetic alopecia: a systematic review. *Cells*. 2023; 12(6): 951.
 11. Tabatabaei Qomi R, Sheykhasan M. Adipose-derived stromal cell in regenerative medicine: a review. *World J Stem Cells*. 2017; 9(8): 107-117.
 12. Giuliano E, Paolino D, Fresta M, Cosco D. Drug-loaded biocompatible nanocarriers embedded in poloxamer 407 hydrogels as therapeutic formulations. *Medicines (Basel)*. 2018; 6(1): 7.
 13. Kamishima T, Hirabe C, Ohnishi T, Taguchi J, Myint KZY, Koga S. Trichoscopic evaluation of dental pulp stem cell conditioned media for androgenic alopecia. *J Cosmet Dermatol*. 2023; 22(11): 3107-3117.
 14. Yuan A, Gu Y, Bian Q, Wang R, Xu Y, Ma X, et al. Conditioned media-integrated microneedles for hair regeneration through perifollicular angiogenesis. *J Control Release*. 2022; 350: 204-214.
 15. Asadi-Golshan R, Razban V, Mirzaei E, Rahmanian A, Khajeh S, Mostafavi-Pour Z, et al. Efficacy of dental pulp-derived stem cells conditioned medium loaded in collagen hydrogel in spinal cord injury in rats: Stereological evidence. *J Chem Neuroanat*. 2021; 116: 101978.
 16. Shaer A, Azarpira N, Aghdaie MH, Esfandiari E. Isolation and characterization of human mesenchymal stromal cells derived from placental decidua basalis; umbilical cord wharton's jelly and amniotic membrane. *Pak J Med Sci*. 2014; 30(5): 1022-1026.
 17. Nekoei SM, Azarpira N, Sadeghi L, Kamalifar S. In vitro differentiation of human umbilical cord Wharton's jelly mesenchymal stromal cells to insulin producing clusters. *World J Clin Cases*. 2015; 3(7): 640-649.
 18. Cespi M, Bonacucina G, Pucciarelli S, Cocci P, Perinelli DR, Casettari L, et al. Evaluation of thermosensitive poloxamer 407 gel systems for the sustained release of estradiol in a fish model. *Eur J Pharm Biopharm*. 2014; 88(3): 954-961.
 19. Zhang Y, Wang X, Chen J, Qian D, Gao P, Qin T, et al. Exosomes derived from platelet-rich plasma administration in site mediate cartilage protection in subtalar osteoarthritis. *J Nanobiotechnology*. 2022; 20(1): 56.
 20. Yang C, Lei D, Ouyang W, Ren J, Li H, Hu J, et al. Conditioned media from human adipose tissue-derived mesenchymal stem cells and umbilical cord-derived mesenchymal stem cells efficiently induced the apoptosis and differentiation in human glioma cell lines in vitro. *Biomed Res Int*. 2014; 2014: 109389.
 21. Noorafshan A, Asadi-Golshan R, Erfanizadeh M, Karbalay-Doust S. Beneficial effects of olive oil on the rats' cerebellum: functional and structural evidence. *Folia Med (Plovdiv)*. 2018; 60(3): 454-463.
 22. Oh HA, Kwak J, Kim BJ, Jin HJ, Park WS, Choi SJ, et al. Migration inhibitory factor in conditioned medium from human umbilical cord blood-derived mesenchymal stromal cells stimulates hair growth. *Cells*. 2020; 9(6): 1344.
 23. Deng W, Zhang Y, Wang W, Song A, Mukama O, Huang J, et al. Hair follicle-derived mesenchymal stem cells decrease alopecia areata mouse hair loss and reduce inflammation around the hair follicle. *Stem Cell Res Ther*. 2021; 12(1): 548.
 24. Sperling LC, Cowper SE, Knopp EA. *An atlas of hair pathology with clinical correlations*. 2nd ed. New York & London: Informa Healthcare; 2012: 216.
 25. Galbraith GM, Thiers BH. In vitro suppression of human lymphocyte activity by minoxidil. *Int J Dermatol*. 1985; 24(4): 249-251.
 26. Choi M, Choi SJ, Jang S, Choi HI, Kang BM, Hwang ST, et al. Shikimic acid, a mannose bioisostere, promotes hair growth with the induction of anagen hair cycle. *Sci Rep*. 2019; 9(1): 17008.
 27. Sintov A, Serafimovich S, Gilhar A. New topical antiandrogenic formulations can stimulate hair growth in human bald scalp grafted onto mice. *Int J Pharm*. 2000; 194(1): 125-134.
 28. Johnson DB, Sonthalia S. FlutamideSeries. In: *StatPearls [Internet]*. StatPearls Publishing; 2021. Available from: <https://www.ncbi.nlm.nih.gov/books/NBK482215/> (1 May 2023).
 29. Ramdasi S, Tiwari SK. Human mesenchymal stem cell-derived conditioned media for hair regeneration applications. *J Stem Cells*. 2016; 11(4): 201-211.
 30. Anudeep TC, Jeyaraman M, Muthu S, Rajendran RL, Gangadaran P, Mishra PC, et al. Advancing Regenerative Cellular Therapies in Non-Scarring Alopecia. *Pharmaceutics*. 2022; 14(3): 612.
 31. Lu H, Poirier C, Cook T, Traktuev DO, Merfeld-Clauss S, Lease B, et al. Conditioned media from adipose stromal cells limit lipopolysaccharide-induced lung injury, endothelial hyperpermeability and apoptosis. *J Transl Med*. 2015; 13: 67.
 32. Jung MK, Ha S, Huh SY, Park SB, Kim S, Yang Y, et al. Hair-growth stimulation by conditioned medium from vitamin D3-activated preadipocytes in C57BL/6 mice. *Life Sci*. 2015; 128: 39-46.
 33. Dong L, Hao H, Xia L, Liu J, Ti D, Tong C, et al. Treatment of MSCs with Wnt1a-conditioned medium activates DP cells and promotes hair follicle regrowth. *Sci Rep*. 2014; 4: 5432.
 34. Li M, Zhong L, He W, Ding Z, Hou Q, Zhao Y, et al. Concentrated conditioned medium-loaded silk nanofiber hydrogels with sustained release of bioactive factors to improve skin regeneration. *ACS Appl Bio Mater*. 2019; 2(10): 4397-4407.
 35. Stortelers C, Kerkhoven R, Moolenaar WH. Multiple actions of lysophosphatidic acid on fibroblasts revealed by transcriptional profiling. *BMC Genomics*. 2008; 9: 387.
 36. Fong CY, Tam K, Cheyyatraivendran S, Gan SU, Gauthaman K, Armugam A, et al. Human Wharton's jelly stem cells and its conditioned medium enhance healing of excisional and diabetic wounds. *J Cell Biochem*. 2014; 115(2): 290-302.
 37. Liu C, Wang C, Yang F, Lu Y, Du P, Hu K, et al. The conditioned medium from mesenchymal stromal cells pretreated with proinflammatory cytokines promote fibroblasts migration and activation. *PLoS One*. 2022; 17(4): e0265049.
 38. Sauter LS, Weibel ER. Morphometric evaluation of skin structures by stereologic methods. Application to testosterone-treated rats. *Dermatologica*. 1971; 143(3): 174-183.
 39. Ban K, Bae S, Yoon YS. Current strategies and challenges for purification of cardiomyocytes derived from human pluripotent stem cells. *Theranostics*. 2017; 7(7): 2067-2077.
 40. Czarnicka A, Odziomek A, Murzyn M, Dubis J, Baglaj-Oleszczuk M, Hryniewicz-Gwóźdź A. Wharton's jelly-derived mesenchymal stem cells in the treatment of four patients with alopecia areata. *Adv Clin Exp Med*. 2021; 30(2): 211-218.